Study of cross sections, oscillator strengths, generalized oscillator strengths, and atomiclike character of the molecular orbitals of formaldehyde for inelastic transitions to valence and Rydberg states*

Kenneth J. Miller

Department of Chemistry, Rensselaer Polytechnic Institute, Troy, New York 12181
(Received 10 September 1974)

Oscillator strengths, generalized oscillator strengths, and cross sections are calculated using Hartree–Fock wavefunctions for spin allowed electronic transitions from the $2b_2(n)$ and $1b_1(\pi)$ molecular orbitals to the nb_2 ($n = 3$, 4, and 5), nb_1 ($n = 2$ and 3) and na_1 ($n = 5,\cdots,10$) Rydberg series, and for the singlet $\rightarrow$ triplet $2b_2) 2b_1)$ transition. The first Born approximation is utilized in the calculation of $f(K)$, and exchange contributions are included in the calculation of the total cross sections with the Born–Ochkur–Rudge modifications. Contour plots illustrating the radial and angular dependence of the orbitals are presented to substantiate the atomiclike character of the nb_2 and nb_1 orbitals and to demonstrate the mixture of atomiclike states which contribute to the na_1 molecular orbitals. The qualitative shape and trends in the occurence of extrema in the generalized oscillator strengths are discussed for transitions to Rydberg series whose excited molecular orbitals possess a given atomiclike character within the same point group symmetry. The oscillator strengths presented agree well with those determined both by electronic scattering techniques and with ultraviolet measurements in all but the $\pi \rightarrow \pi^*$ excitation.

INTRODUCTION

The electronic structure of formaldehyde is being extended with high resolution ultraviolet spectroscopy[1,2] as well as with electron scattering spectroscopy.[3] Although the resolution in optical spectroscopy (~0.5 Å, $\delta E \approx 0.0008$ eV at 3000 Å) is much better than electron spectroscopy ($\delta E \sim 0.02$ eV), the latter provides two additional degrees of freedom when taking an energy loss spectrum; at low incident energies, optically forbidden transitions appear, and in studies where the scattering angle is varied, the scattered electron intensity exhibits unique behavior for excitations to Rydberg series with a given atomiclike symmetry in the same point group symmetry. Thus, transitions to the different electronic states of molecules can be identified both through the position in the spectrum as well as by the angular dependence of the differential cross sections.

In recent years measurements of inelastic differential cross sections of electrons scattered off polyatomic molecules have revealed interesting features in the behavior of the generalized oscillator strength $f(K)$ as a function of momentum transfer K.[4] Theoretically, the generalized oscillator strength calculated within the first Born approximation is

$$\frac{f_{if}(K)}{\Delta E} = 2\omega \int \frac{d\Omega}{4\pi} \frac{|(\Psi_f|\sum_\mu e^{i\mathbf{K}\cdot\mathbf{r}_\mu}|\Psi_i)|^2}{K^2}, \qquad (1)$$

where Ψ_i and Ψ_f are the initial and final electronic wavefunctions, and ω the degeneracy of the excited state. The vibrational and rotational contributions have been summed, resulting in an integral average over all molecular orientations for vertical transitions from the ground equilibrium state.

In the present investigation, electronic transitions in formaldehyde from the $1b_1$ (π) and $2b_2$ (n) molecular orbitals to the Rydberg series nb_2 ($n = 3$, 4, and 5), nb_1 ($n = 2$ and 3), and na_1 ($n = 5, \ldots, 10$) are studied to examine the shape of $f(K)$ for dipole allowed and quadrupole type transitions. Recent studies of generalized oscillator strengths as a function of momentum transfer in atomic systems have revealed that the extrema in $f(K)$ occur at approximately the same value of K for transitions to the same Rydberg series and that the positioning of these extrema are unique to the particular transitions studied.[5] Contour plots of the molecular orbitals participating in the one-electron transitions in CH_2O are presented. The atomiclike character of the b_1 and b_2 orbitals is obvious owing to their orientation perpendicular to the C=O axis, whereas the a_1 molecular orbitals contain mixtures of s, p, and d atomiclike orbitals. In this paper molecular orbitals are assigned an atomiclike character, and trends in the qualitative shape of $f(K)$ are examined. To uniquely assign the principal quantum number in each of the atomiclike designations, the quantum defects are evaluated and each of the molecular orbitals in CH_2O are related to their counterparts in O_2. One exception to the accepted classification occurs in the npa_1 Rydberg molecular orbitals; the $7a_1$ orbital in this paper is associated with the $4pa_1$ rather than the usual $3pa_1$ orbital. This assignment permits an association of the inner molecular orbitals in formaldehyde with the required number of npa_1 ($n \leq 3$) atomiclike states for the inner core orbitals. The problem of proper assignment of principal quantum numbers for the very deeply penetrating molecular orbitals of σ symmetry has already been discussed in the case of the homonuclear diatomic molecules N_2 and O_2 by Miller and Green.[6]

Hartree–Fock wavefunctions whose molecular orbitals consist of linear combinations of Gaussian-type functions are those determined by Mentall *et al.*[2] The ground

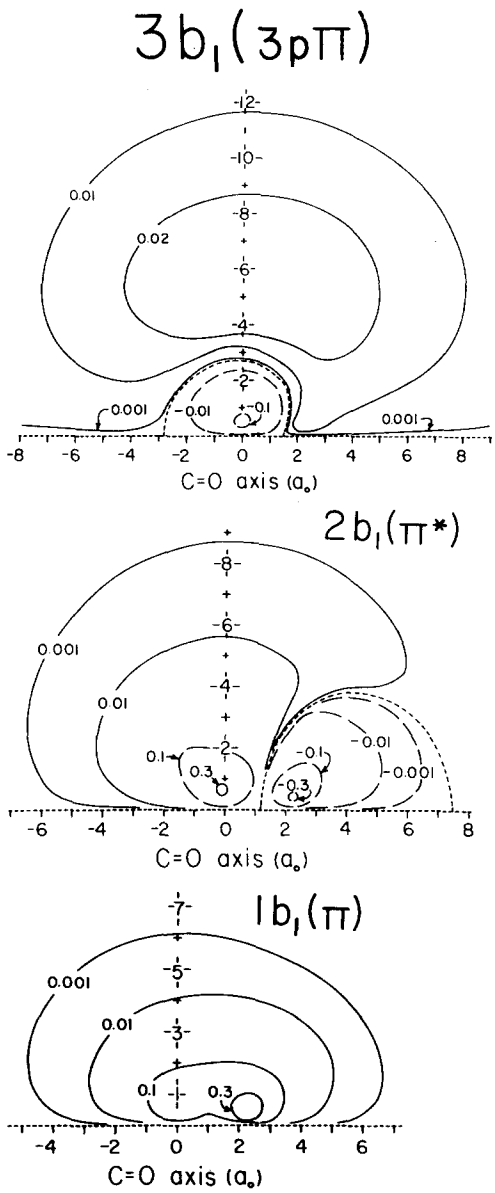

FIG. 1. $1b_1$ ($2p\pi$) valence, $2b_1$ ($3d\pi^*$) antibonding valence, and $3b_1$ ($3p\pi$) Rydberg molecular orbitals plotted in the C=O–x plane.

state configuration in order of increasing energy is

$$1a_1^2 2a_1^2 3a_1^2 4a_1^2 5a_1^2(\sigma) 1b_2^2 1b_1^2(\pi) 2b_2^2(n)\,,$$

where the usual designations are given to the $5a_1$, $1b_1$, and $2b_2$ orbitals. The excited states are first obtained by solving the SCF (self-consistent-field) equations for the ion, and then solving the open shell equations for the added electron in the frozen ion core field. Therefore the set of Rydberg solutions are orthogonal to each other, and the eigenvalues are then the Rydberg term values measured relative to the ion energy. For the quadrupole transitions within a given symmetry type, the Rydberg molecular orbitals were Schmidt orthogonalized to the occupied valence orbitals of the initial or ground state. This procedure ensures that $f(K)$ vanishes at $K = 0$. The occupied orbitals of the ion core and the neutral species are sufficiently close, as determined by a calculation of the overlap between the two sets of orbitals, so that one-electron transitions may be considered out of each occupied pair; that is, a two electron valence state singlet coupled wavefunction is used.

TABLE I. Coordinate positions in Bohr radii (a_0) for CH_2O.

Atom	Axis C=O	y	$x(\pi)$
C	0.0	0.0	0.0
O	2.2866	0.0	0.0
H_1	−1.8134	−1.0239	0.0
H_2	−1.8134	1.0239	0.0

CONTOUR PLOTS OF MOLECULAR ORBITALS

The qualitative shape of the generalized oscillator strengths for atomic systems depends on the symmetry of the orbitals participating in the transitions. In Figs. 1–4 the contour plots of the molecular orbitals reveal their somewhat atomiclike appearance, and this idea is utilized in the analysis. The geometry of CH_2O is implied by the atomic positions given in Table I. Within the convention used in this paper, the *pi* orbitals are of b_1 symmetry.

In Fig. 1, the nb_1 orbitals are shown. The large nuclear charges of the carbon and oxygen atoms govern the shapes of the molecular orbitals. The $1b_1$ MO is clearly a $2p\pi$ orbital shifted toward the oxygen atom. The $2b_1$ MO is an antibonding *pi* orbital or a distorted $3d\pi^*$ atomic orbital centered approximately midway between carbon and oxygen. Both molecular orbitals are valence in character, as seen by comparison with the $5a_1$ and $2b_2$ valence orbitals presented in Figs. 2 and 3. The $3b_1$ orbital is clearly of Rydberg character; its outer lobe has a maximum at $x \approx 6a_0$, which is well beyond the extent of the valence orbitals. From the contour plot it is clear that this orbital is very much like a $3pb_1$ atomic orbital centered on the carbon atom.

In Fig. 2, the nb_2 ($n = 1, \ldots, 5$) molecular orbitals are shown. The influence of the hydrogen atoms on the outer valence and Rydberg orbitals is small, and the

TABLE II. Valence and Rydberg molecular orbitals in CH_2O, their atomiclike character, and theoretical quantum defects.

MO	AO type	δ[a]
$1b_1$	π	0.97
$2b_1$	$\pi^*(3d)$	0.86
$3b_1$	$3p$	...
$2b_2$	$3d$	1.78
$3b_2$	$3p$	0.83
$4b_2$	$4d$	1.02
$5b_2$	$4p$	0.67
$5a_1$	$3d\sigma$	2.07
$6a_1$	$3sa_1$	1.09
$7a_1$	$4pa_1$	1.83
$8a_1$	$4s$	1.03
$9a_1$	$4d\sigma$	0.92
$10a_1$	$3d\delta$	1.90

[a]Quantum defects obtained from theoretical data.

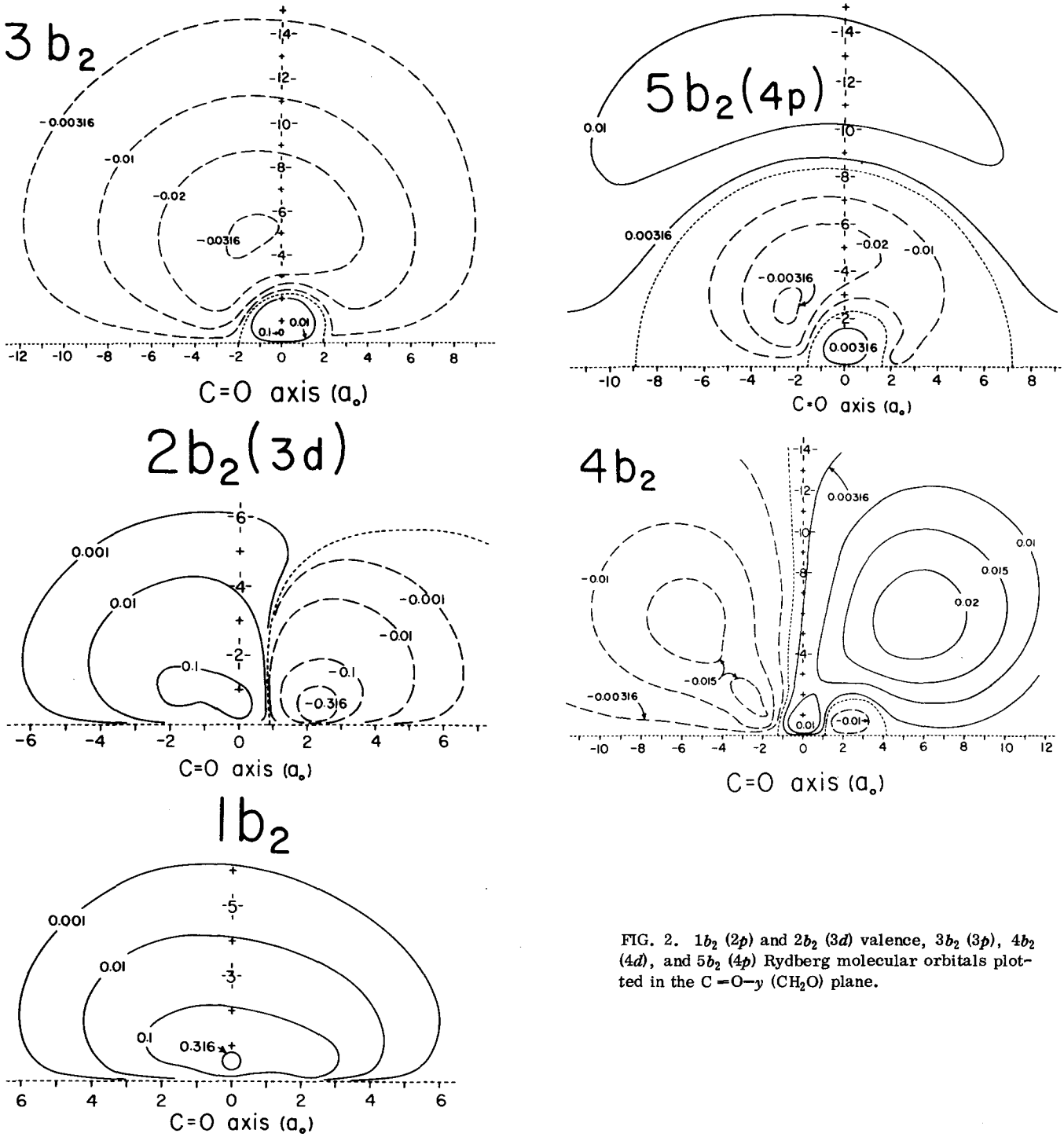

FIG. 2. $1b_2$ ($2p$) and $2b_2$ ($3d$) valence, $3b_2$ ($3p$), $4b_2$ ($4d$), and $5b_2$ ($4p$) Rydberg molecular orbitals plotted in the C=O–y (CH_2O) plane.

near degeneracy of the b_1 and b_2 orbitals is apparent. The $1b_2$ valence orbital is of $2p$ character, but, unlike its $1b_1$ counterpart, it is centered about the carbon atom. The $2b_2$ ($3d$) and $3b_2$ ($3p$) molecular orbitals have their counterparts in the $2b_1$ and $3b_1$ orbitals, respectively, being centered, respectively, between the carbon and oxygen atoms and about the carbon atom. In the case of the $4b_2$ Rydberg orbital, the differing number of radial nodes in each angular lobe suggests an orbital with character between a $3d$ and $4d$ atomiclike orbital. From the quantum defect ($\delta = 1.02$) given in Table II, as well as the extent of this orbital, it will be referred to as a $4d$ orbital, although a hybrid mixture would no doubt more accurately represent this case. The $5b_2$ MO is of $4p$ nature ($\delta = 0.67$), and its extent into the next quantum level is apparent from the maximum in the outer lobe which occurs at $y \approx 12a_0$.

In Fig. 3, orbitals of a_1 symmetry are shown. Their orientation along the C=O axis results in a large interaction with the carbon and oxygen atoms, unlike the b_1 and b_2 MO's. The atomiclike appearance of these orbit-

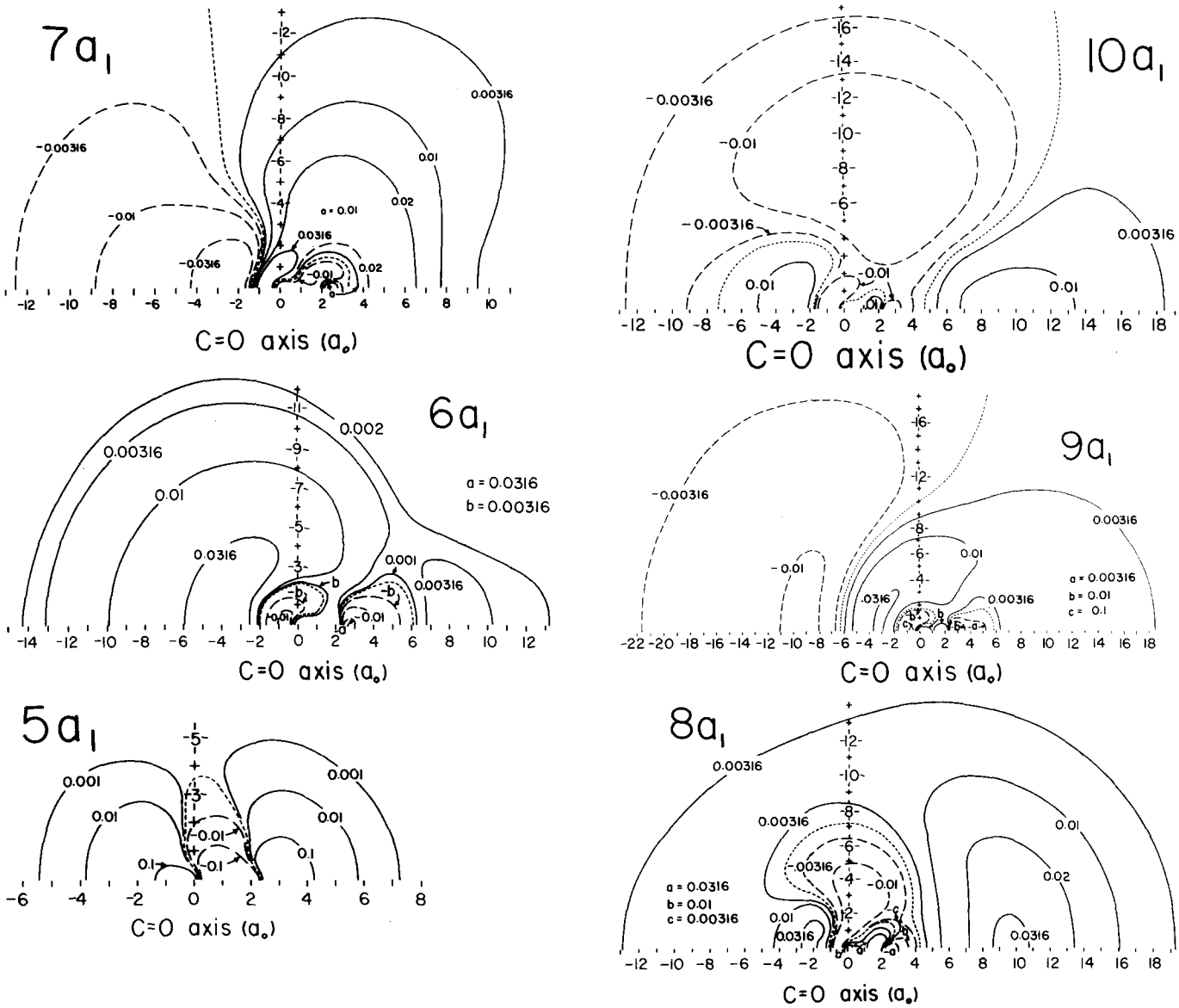

FIG. 3. $5a_1$ ($3d\sigma$) valence, $6a_1$ ($3s$), $7a_1$ ($4p$), $8a_1$ ($4s$), $9a_1$ ($4d\sigma$), and $10a_1$ ($3d\delta$) Rydberg orbitals plotted in the C=O–y (CH_2O) plane.

als is somewhat lost, and even the resemblance to their analogues in O_2 is difficult to recognize in the higher Rydberg states. The $5a_1$ valence molecular orbital takes on the $3d$ appearance similar to the $3\sigma_g$ orbital in oxygen. The $6a_1$ and $8a_1$ molecular orbitals resemble distorted in-phase linear combinations of s-type atomic orbitals on carbon and oxygen, but clearly there is no character in these which can be interpreted as p-type centered in the central molecular region. These are assigned sa_1 character. On the other hand, the $7a_1$, $9a_1$, and $10a_1$ orbitals have a node which intersects the molecule perpendicular to the C=O axis which displays a p-type character in the Rydberg region, but a d-type orbital in the valence region.

The presence of $d\delta$ character in the $10a_1$ molecular orbital is established by an examination of the contour plot in the $x(\pi)$–y plane through the carbon atom shown in Fig. 4. Contour plots of the $5a_1$ through the $9a_1$ molec-

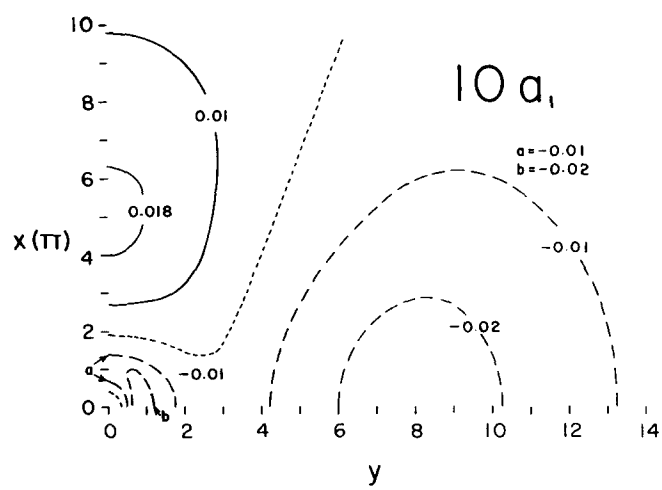

FIG. 4. $10a_1$ ($3d\delta$) Rydberg orbital plotted in the $x(\pi)$–y plane through the C atom.

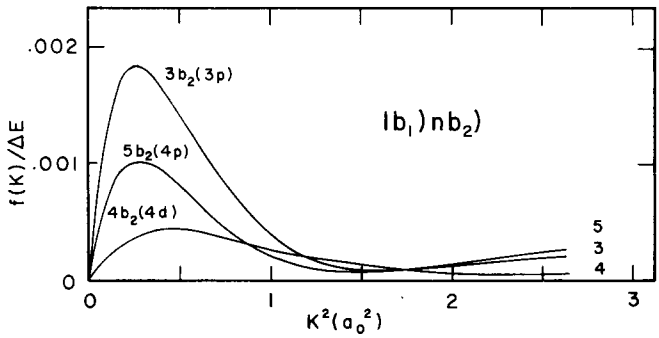

FIG. 5. Generalized oscillator strengths for the $1b_1)nb_2)$ excitations.

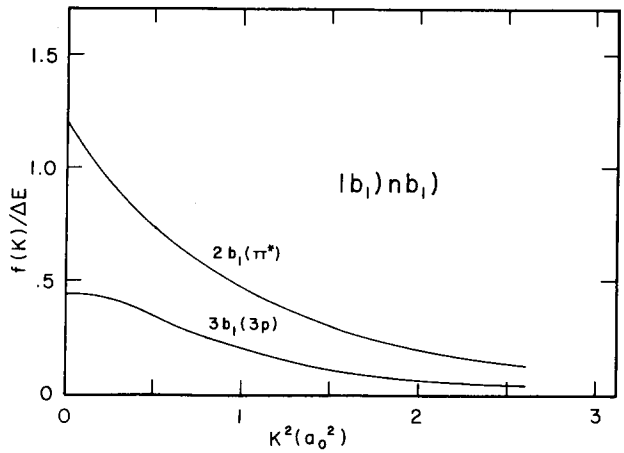

FIG. 7. Generalized oscillator strengths for the $2b_2)nb_1)$ excitations.

ular orbitals (not shown) in the $x(\pi)$–y plane show the $5a_1$, $6a_1$, and $7a_1$ molecular orbitals to be nearly cylindrically symmetrical about the C=O axis. The $8a_1$ orbital is elongated along the $x(\pi)$ axis and the $9a_1$ orbital is elongated along the y axis. Therefore all but the $10a_1$ are characterized by σ rather than δ symmetry.

Assignment of the atomiclike character of the na_1 ($n = 5, \ldots, 9$) will now be confirmed on the basis of quantum defect. By accounting for all the core and valence electrons within an independent particle model utilizing the united atom notation, the quantum numbers and hence quantum defects of the Rydberg orbitals in O_2 were assigned in a nonarbitrary manner by Miller and Green.[6] They found quantum defects of 1.06 for the ns series, 1.7 and 0.5 for the $np\sigma$ and the $np\pi$ series, and 1.18 and 1.11 for the $nd\sigma$ and $nd\pi$ series, respectively. The integer difference in the quantum defect of the σ and π np series is explained by the deep penetration of the sigma molecular orbitals; this effect becomes more pronounced as the nuclear charge increases, as seen in H_2, N_2, and O_2. Correspondence between the molecular orbitals in formaldehyde and in the oxygen molecule suggests that the $7a_1$ orbital ought to be assigned the $4pa_1$ atomiclike character with quantum defect of 1.83 and not to the $n = 3$ quantum level, thus leaving $n \leq 3$ for the occupied orbitals. In Fig. 3, the $7a_1$ orbital exhibits two radial nodes which also supports this assignment. The $9a_1$ orbital exhibits $3d$ character in the molecular region, but the appearance of a node perpendicular to the C=O axis suggests p character, the net result being a mixture of p- and d-type orbitals. Based on a theoretical determination of quantum defects reported in Table II, the $9a_1$ molecular orbital is labelled $4d\sigma$. Quantum defects for the ns series suggest that the $6a_1$ ($\delta = 1.09$) and $8a_1$ ($\delta = 1.03$) molecular orbitals, respectively, be assigned the $3sa_1$ and $4sa_1$ atomiclike orbitals, and this choice is supported by the contour plots shown in Fig. 3.

The $5a_1$ ($3d$) and $2b_2$ ($3d$) molecular orbitals with quantum defects of 2.07 and 1.78, respectively, are much larger than those for each of their respective series; however, the large interaction with the nuclei along the C=O axis and in the H_2C plane produces these very penetrating orbitals. The quantum defect of the $1b_1$ orbital, however, corresponds to that expected from the $p\pi$ series. The present assignments not only correspond to quantum defects of the molecular orbitals in CH_2O, but also give rise to a consistent notation which connects these molecular orbitals with atomiclike counterparts, especially in the case of Rydberg orbitals on which a great deal of our understanding of molecular spectroscopy is based.

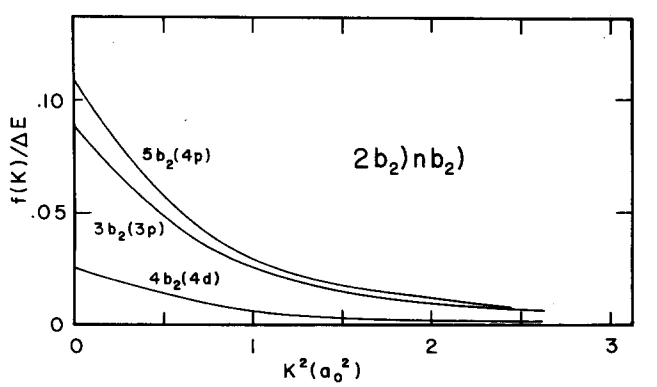

FIG. 6. Generalized oscillator strengths for the $2b_2)nb_2)$ excitations.

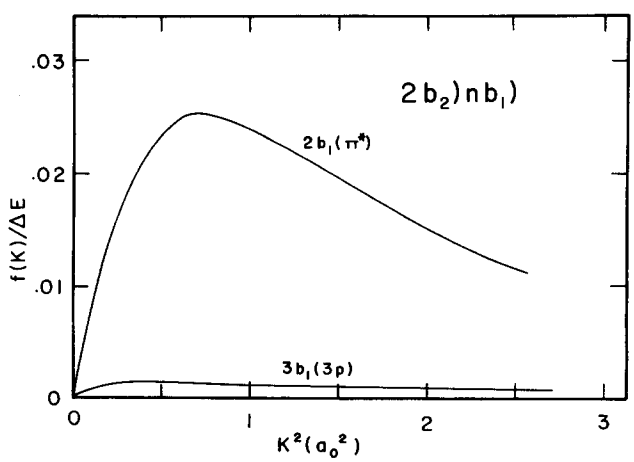

FIG. 8. Generalized oscillator strengths for the $1b_1)nb_1)$ excitations.

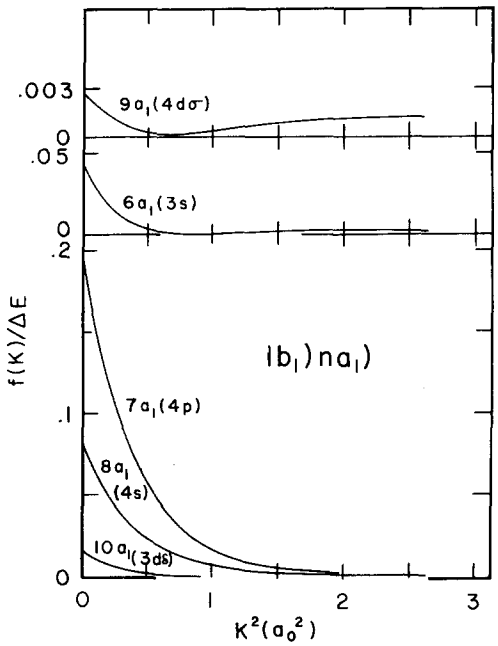

FIG. 9. Generalized oscillator strengths for the $1b_1)na_1)$ excitations in CH_2O.

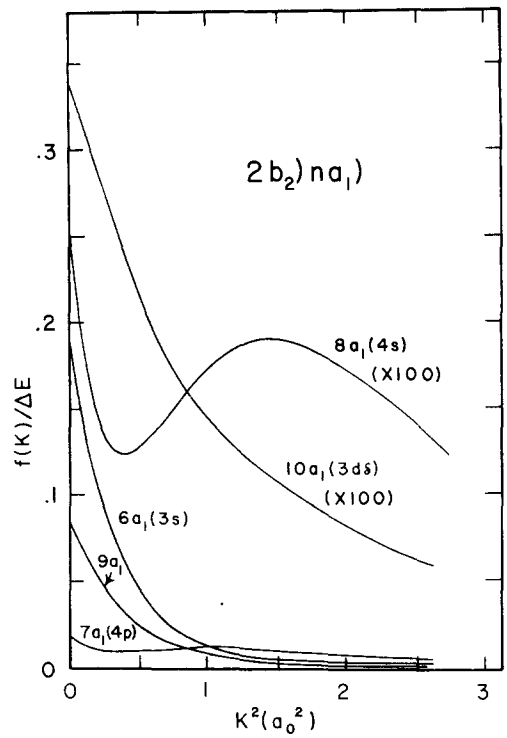

FIG. 10. Generalized oscillator strengths for the $2b_2)na_1)$ excitations.

TRENDS IN THE APPEARANCE OF EXTREMA IN $f(K)$

Recent studies of the qualitative shape of $f(K)$ vs K in atomic systems have shown that extrema in $f(K)$ occur at larger values of K as the principal quantum number increases, but nevertheless, they occur at approximately the same values of K for all members of a given Rydberg series[5]; the greatest deviation occurs for the valence state excitations. The qualitative shape of the generalized oscillator strengths depends on the space and spin symmetry of the orbitals participating in the transition. For atomic transitions, the dependence is on angular momentum. In the case of molecular transitions, each excited symmetry orbital falls into one of the angular momentum classifications according to its atomiclike behavior. For formaldehyde, this behavior is given in Table II.

In Fig. 5, the generalized oscillator strengths are shown for transitions into the nb_2 Rydberg series from the $1b_1$ (π) orbital. In this case, both the npb_2 and the ndb_2 curves shown exhibit the same qualitative shape. An extrapolation of $f(K)/\Delta E$ curves to higher quantum levels should yield curves of the same qualitative shape but attenuated by $(n-\delta)^{-3}$. The extrema in $f(K)$ appear at $K^2 = 0.26$ and 0.28, respectively, for transitions to the $3b_2$ ($3p$) and the $5b_2$ ($4p$) Rydberg orbitals, whereas $K^2 = 0.46$ for a transition to the $4b_2$ ($3d$) orbital. These

TABLE III. Oscillator strengths for the optically allowed $2b_2)na_1)$, $2b_2)nb_2)$, $1b_1)na_1)$, and $1b_1)nb_1)$ transitions in CH_2O.[a]

Transition	Type	ΔE[b]	f_D(th)	f_v(th)	f(es)	f(uv)
$2b_2)6a_1)$	$3sa_1$	7.10(0.261)	0.0508	0.0365	0.028	0.038
$3b_2)$	$3pb_2$	7.98(0.293)	0.0261	0.0208	0.017	0.017 ± 0.002
$7a_1)$	$4pa_1$	8.14(0.299)	0.0057	0.0093	0.032	0.038 ± 0.004
$4b_2)$	$4db_2$	8.88(0.326)	0.0083	0.0075	0.015	0.010 ± 0.003
$8a_1)$	$4sa_1$	9.20(0.332)	0.0009	0.0003	···	···
$9a_1)$	$4d\sigma$	9.03(0.338)	0.0293	0.0155	0.017	0.012 ± 0.004
$5b_2)$	$4pb_2$	9.65(0.355)	0.0390	0.0265	0.032	0.028 ± 0.003
$10a_1)$	$3d\delta$	9.05(0.333)	0.0011	0.0008	···	···
$1b_1)6a_1)$	$3sa_1$	10.70(0.393)	0.0175	0.0229	···	···
$7a_1)$	$4pa_1$	11.30(0.415)	0.0829	0.0499	···	···
$8a_1)$	$4sa_1$	12.70(0.467)	0.0389	0.0237	···	···
$9a_1)$	$4d\sigma$	12.20(0.448)	0.0012	0.0022	···	···
$10a_1)$	$3d\delta$	12.22(0.449)	0.0075	0.0098	···	···
$1b_1)2b_1)$	π^*	11.31(0.415)	0.499	0.199	neg.	neg.
$3b_1)$	$3pb_1$	12.80(0.470)	0.0206	0.0093		

[a]Oscillator strengths are obtained from the present theoretical work (th), the electron scattering (es) results of Ref. 3, and the vacuum ultraviolet spectra (uv) of Ref. 2.
[b]ΔE = energy lost in eV and a.u. obtained from Fig. 1 of Ref. 3.

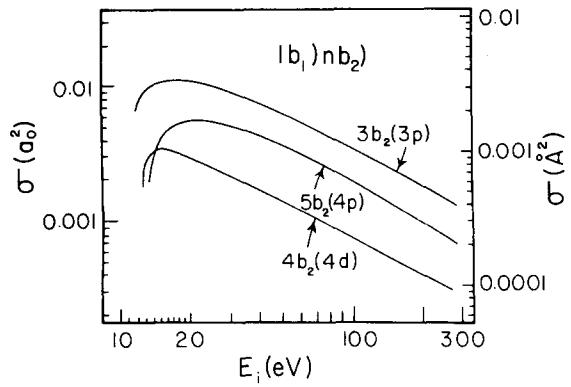

FIG. 11. Total cross sections for the $1b_1)nb_2)$ singlet → singlet excitations.

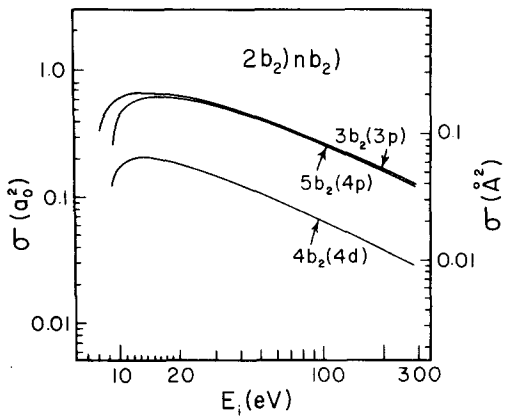

FIG. 12. Total cross sections for the $2b_2)nb_2)$ singlet → singlet excitations.

results support the conjecture, verified in the atomic case, that the qualitative shape and positioning of the extrema are the same for transitions to members of a given angular momentum symmetry type in a Rydberg series. Transitions to the nb_2 orbitals from the $2b_2$ orbital once again yield $f(K)/\Delta E$ curves that are qualitatively similar for both the npb_2 and ndb_2 transitions as is shown in Fig. 6.

Transitions to the nb_1 series from the $1b_1$ and $2b_2$ molecular orbitals are shown in Fig. 7 and 8. That $f(K)/\Delta E$ differs for transitions to the $2b_1$ ($3d \sim \pi^*$) and the $3b_1$ ($3p$) molecular orbitals can probably be explained by the different atomic symmetry character of each of these orbitals. If the positioning of the extrema for transition to members of a given series is characteristic of the atomiclike angular symmetry, then the position of the extrema $K^2 = 0.70$ for the $2b_2)2b_1)$ transition can be assumed to be the same as those for transitions to their respective ndb_1 and the npb_1 Rydberg series. To extrapolate to the higher members of the respective Rydberg series, one would merely adjust $f(K)$ by $(n-\delta)^{-3}$, in analogy to the n^{-3} rule for the oscillator strengths of hydrogen. The $1b_1)nb_1)$ transitions exhibit no extrema, and the shape of the curves differ somewhat. Here once again, transitions to the Rydberg series ndb_1 and npb_1 could be obtained by scaling $f(K)$.

Transitions to the na_1 Rydberg series are the most difficult to interpret because the molecular orbitals are mixtures of s, p, and d atomiclike σ- and δ-type orbitals of a_1 symmetry, and each yields results dependent on the state from which an electron is being excited. For example, the $6a_1$ and $9a_1$ molecular orbitals both exhibit "$3da_1$" character in the valence region about the oxygen atom, namely, where the $1b_1$ orbital is centered and confined. On the other hand, the $7a_1$ and $8a_1$ molecular orbitals exhibit "p" character in the valence region about the midpoint between the C=O bond, that is, where the node in the $2b_2$ molecular orbital is centered. It is on this basis that the appearance of minima in $f(K)$ for the $1b_1)na_1)$ ($n = 6$ and 9) transitions shown in Fig. 9, and for the $2b_2)na_1)$ ($n = 7$ and 8) transitions shown in Fig. 10, can be understood rather than on the overall gross atomiclike character of the na_1 Rydberg orbitals.

In the $1b_1)na_1)$ transitions, the orbitals for which $n = 7$ and 8 are of "p" character in the region about the oxygen atom, and similarly, in the $2b_2)na_1)$ transitions, the orbitals for which $n = 6$ and 9 are similar about the midpoint of the C=O bond.

Notwithstanding this qualitative analysis of transitions to the na_1 series, it is clear that molecular orbitals which interact strongly with atomic nuclei display mixtures whose atomiclike character depends strongly upon the space overlap with the initial state. That the analysis is straightforward in the case of the transitions among the nb_1 and nb_2 states is understood by noting that these orbitals with nodal planes through the C=O axis are not very penetrating; the small nuclear charge of the hydrogen atoms do not greatly affect the nb_2 molecular orbitals.

OSCILLATOR STRENGTHS

Oscillator strengths for the excitations studied in formaldehyde are reported in Table III. Theoretical values compare well with the experimental values obtained from electron scattering[3] and ultraviolet spectra[2] in all cases except the $1b_1)2b_1)$, or $\pi \rightarrow \pi^*$ transition. Experimental studies suggest a negligible value, whereas theoretical calculations yield $f = 0.199$ with Hartree–Fock wavefunctions. Whitten and Hackmeyer[7] obtain

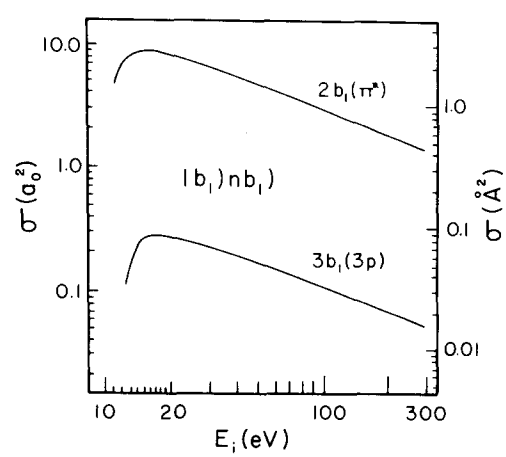

FIG. 13. Total cross sections for the $1b_1)nb_1)$ singlet → singlet excitations.

TABLE IV. Estimated transition energies for the optically forbidden $1b_1)nb_2)$ and $2b_2)nb_1)$ transitions.[a]

MO	Rydberg energy (eV)	Estimated transition energy (eV)[b]
	$(I.P.)_1 - \Delta E[2b_2)nb_2)] = \epsilon(nb_2)$	$(I.P.)_2 - \epsilon(nb_2) \cong \Delta E[1b_1)nb_2)]$
$3b_2$	2.90	11.17
$4b_2$	2.00	12.07
$5b_2$	1.23	12.84
	$(I.P.)_2 - \Delta E[1b_1)nb_1)] = \epsilon(nb_1)$	$(I.P.)_1 - \epsilon(nb_1) \cong \Delta E[2b_2)nb_1)]$
$2b_1$	2.76	8.12 (3.49)
$3b_1$	1.27	9.61

[a] $(I.P.)_1 = 10.88$ eV, $(I.P.)_2 = 14.07$ eV.
[b] $\Delta E[2b_2)2b_1)] = 3.49$ eV for the experimental singlet → singlet excitation.

a value of $f = 0.4$ using a configuration interaction wavefunction with over three hundred terms. Theoretical calculations by Whitten and Hackmeyer and Peyerimhoff *et al.*[8] for excitations from the $2b_2$ molecular orbital to the 3s and 3p Rydberg states show that these are predominantly valence in character; they are categorized as $\pi \rightarrow \pi^*\ ^1A_1$, and $\sigma \rightarrow \pi^*\ ^1B_1$, respectively. The $^1A_1$ state in both calculations is found to lie above the $^2B_2$ ionization limit, which suggests a strong mixing with the continuum of the ndb_2 series and hence the possibility of autoionization. Model calculations with CI (configuration interaction) wavefunctions by Mentall *et al.*[2] in which the $\pi \rightarrow \pi^*\ ^1A_1$ valence configuration is allowed to mix with the $2b_2 3db_2$ Rydberg $^1A_1$ configuration showed a significant mixing (30%) with this and all members of the ndb_2 configurations; however, the negligible oscillator strength obtained experimentally is as yet still unexplained.

Although the $\pi \rightarrow \pi^*\ \{1b_1)2b_1)\}$ transition has no minimum in $f(K)$, the large mixing of the $1b_1)2b_1)$ configuration with the $2b_2)ndb_2)$ series reported by Mentall *et al.*[2] suggests that $f(K)$ too is diluted throughout the continuum and thus becomes negligible. In the case of ethylene, Krauss and Mielczarek[9] obtained a minimum in $f_{\text{exptl}}(K)$,

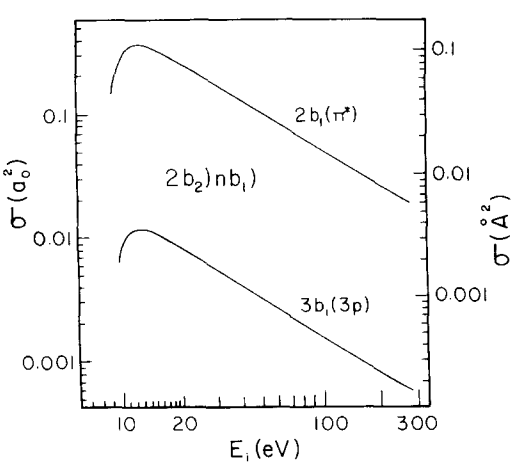

FIG. 14. Total cross sections for the $2b_2)nb_1)$ singlet → singlet excitations.

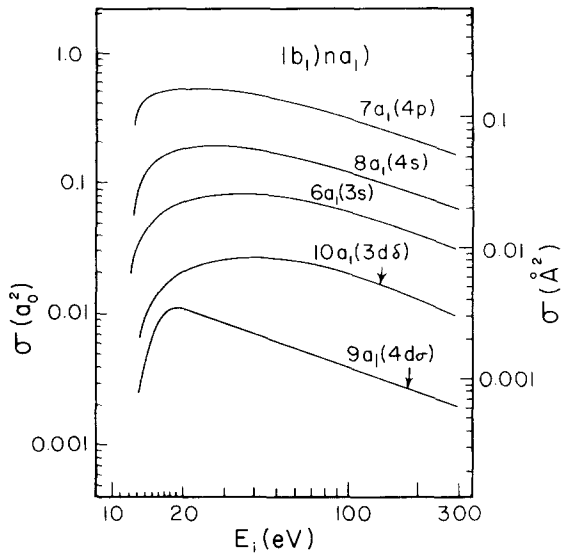

FIG. 15. Total cross sections for the $1b_1)na_1)$ singlet → singlet excitations.

whereas Miller's[10] calculation with Hartree–Fock wavefunctions yielded none. A configuration interaction calculation for the $\pi \rightarrow \pi^*$ transition would probably yield generalized oscillator strengths with minima, which would be introduced through large mixing with excited Rydberg configurations. The valence transitions are the most difficult to study because correlation within the unfilled shells changes drastically between valence and low lying Rydberg transitions. For larger quantum numbers, the npb_2 and npa_1 series occur at the same energy, so that a total theoretical value of 0.0304 obtained from the sum of the $9a_1$ and $10a_1$ must be compared with the experimental value of $f(\text{es}) = 0.017$.

TABLE V. Total cross sections (a_0^2) for valence and Rydberg transitions in CH_2O at selected energies.

Transition	Energy (eV) 100	500	1000	5000
$1b_1)6a_1)$	0.0685	0.0259	0.0156	0.0044
$7a_1)$	0.3813	0.1322	0.0781	0.0212
$8a_1)$	0.1471	0.5261	0.0313	0.0086
$9a_1)$	0.0049	0.0018	0.0011	0.0003
$10a_1)$	0.0234	0.0093	0.0056	0.0016
$2b_2)6a_1)$	0.5052	0.1560	0.0898	0.0234
$7a_1)$	0.0566	0.0170	0.0097	0.0025
$8a_1)$	0.0078	0.0023	0.0013	0.0003
$9a_1)$	0.2014	0.0648	0.0376	0.0099
$10a_1)$	0.0108	0.0032	0.0018	0.0005
$1b_1)3b_2)$	0.0039	0.0009	0.0004	0.0009
$4b_2)$	0.0008	0.0002	0.0001	0.0000_2
$5b_2)$	0.0022	0.0005	0.0003	0.0000_5
$1b_1)2b_1)$	3.218	0.9989	0.5733	0.1484
$3b_1)$	0.1225	0.0381	0.0218	0.0056
$2b_2)3b_2)$	0.2724	0.0805	0.0457	0.0116
$4b_2)$	0.0724	0.0219	0.0125	0.0032
$5b_2)$	0.3000	0.0924	0.0530	0.0137
$2b_2)2b_1)_T$	0.0791	0.0134	0.0065	0.0013
$2b_2)2b_1)$	0.0578	0.0124	0.0063	0.0013
$3b_1)$	0.0020	0.0004	0.0002	0.0000_4

TOTAL CROSS SECTIONS

Total inelastic cross sections for the valence and Rydberg states in formaldehyde already studied are presented in Figs. 11–17. They are calculated by considering one electron excitation out of an occupied pair, i.e., $a)^2 \rightarrow a)b)$ type. The exchange contributions are included through the Bonham,[11] Ochkur,[12] and Rudge[13] approximations and modifications which yield a total cross section

$$\sigma = \frac{4\pi}{k_i^2} \int_{K_{min}}^{K_{max}} \left| \left\{ d + \frac{eK^2}{(k_f - i\sqrt{2I})^2} \right\} \right|^2 \frac{f(K)}{\Delta E} \frac{dK}{K}, \qquad (2)$$

where $f(K)$ [Eq. (1)] is the generalized oscillator strength calculated without exchange and I is the ionization potential. The respective coefficients $d = 1$ and $e = 1/2$ account for the direct and exchange contributions for singlet → singlet transitions, and $d = 0$ and $e = \sqrt{3}/2$ account for singlet → triplet transitions. In this investigation, experimental excitation energies, listed in Table III, were utilized for the optically allowed transitions.

Estimates of the excitation energies for the optically forbidden transitions $1b_1)nb_2)$ and $2b_2)nb_1)$ were made by first calculating the orbital energy from the ionization potential and the excitation energy of the appropriate optically allowed transition, and then subtracting this orbital energy from the appropriate ionization potential. These results, summarized in Table IV, were employed in the cross section calculations for all but the $2b_2)2b_1)$ singlet → singlet transition for which the available experimental result was used. These estimates should be accurate for excitations to high lying Rydberg orbitals. The fact that both the $2b_2$ and $2b_1$ MO's are of $3d$ character [the $2b_1$ (π^*) being more diffuse] suggests that $\Delta E[2b_2)2b_1)] = 8.12$ eV is too large, and this deduction is supported by the experimental value of 3.49 eV. For the singlet → triplet $2b_2)2b_1)$ transition, calculation of the total cross sections were made using the experimental ΔE of 3.12 eV. That transitions to these singlet (3.49 eV) and triplet (3.12 eV) states

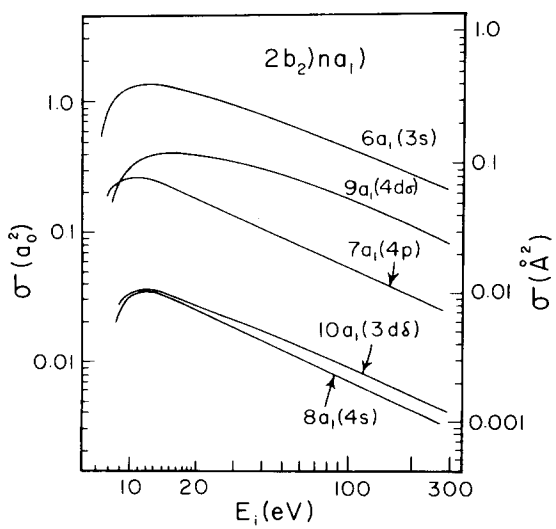

FIG. 16. Total cross sections for the $2b_2)na_1)$ singlet → singlet excitations.

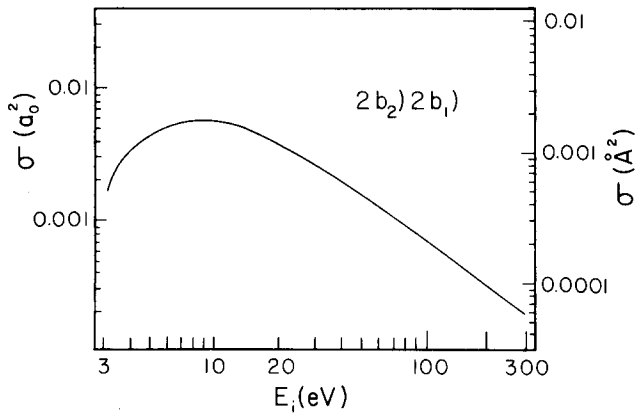

FIG. 17. Total cross sections for the $2b_2)2b_1)$ singlet → triplet excitation.

are well separated from the allowed transitions in the spectrum suggests electron spectroscopy as a suitable technique to study these states. In Figs. 11 and 12, cross sections are presented for the $1b_1 \rightarrow nb_2$ and $2b_2 \rightarrow nb_2$ transitions. That the transition to the $4b_2$ molecular orbital is out of order is understood on the basis of its symmetry; namely, the $3b_2$ and $5b_2$ are of p symmetry and the $4b_2$ is of d symmetry.

In Figs. 13 and 14, the cross sections for transitions to the nb series are presented, the $2b_1$ and $3b_1$ being of d and p symmetries, respectively. In Figs. 15 and 16, cross sections for the $1b_1)na_1)$ and $2b_2)na_1)$ transitions illustrate well the lack of dependence of the MO's on the point group symmetry. In fact, the dependence on atomiclike symmetry is not straightforward in these cases. For example, cross sections for the $3s$ ($6a_1$) and $4s$ ($8a_1$) MO's are ordered as expected in the $1b_1)na_1)$ excitation, whereas they are inverted in the $2b_2)na_1)$ case. This may be understood on the basis that each of these orbitals is not purely an s orbital. The $6a_1$ appears to have some $p\sigma$ character, whereas the $8a_1$ MO is somewhat d-like. For this reason, one must conclude that the orbitals of a_1 symmetry in CH_2O, and very likely those orbitals which lie along the principal axis in any molecular species, will not fit easily into any scheme of analysis needed to rationalize the dependence of molecular properties on atomiclike or molecular quantum numbers. Because the dependence of $\log\sigma$ on $\log E_i$ is nearly linear for large incident energies, the cross sections at representative values of E_i up to 5000 eV are tabulated in Table V for the states studied in this investigation.

CONCLUSION

This investigation of generalized oscillator strengths and total cross sections demonstrates qualitatively a relationship with the atomiclike character of the molecular orbitals participating in the electronic transition. MO's of b_1 and b_2 symmetry show strong atomic character and trends in $f(K)$ and σ appear for each of the pb_1 and db_1, and pb_2 and db_2 series. Those of a_1 symmetry orientated along the internuclear axis appear to contain mixtures of s, p, and d atomiclike contributions, and

consequently, the trends within the "sa_1," "pa_1," and "da_1," series are not always consistent. This is explained by noting that the atomiclike character of the orbital in the valence region may differ from that in the Rydberg region. Consequently, the symmetry of the initial orbital type is important in the calculation of one-electron properties and must be considered in the interpretation of spectral properties.

*Work supported by the Petroleum Research Foundation of the American Chemical Society, Grant Number PRF 5642 AC5.

[1]G. Fleming, M. M. Anderson, A. J. Harrison, and L. W. Pickett, J. Chem. Phys. 30, 351 (1959).
[2]J. E. Mentall, E. P. Gentieu, M. Krauss, and D. Neumann, J. Chem. Phys. 55, 5471 (1971).
[3]M. J. Weiss, C. E. Kuyatt, and S. Mielczarek, J. Chem. Phys. 54, 4147 (1971).
[4]See, for example, the review article by E. N. Lassettre, Can. J. Chem. 47, 1733 (1969). Also Y. K. Kim, M. Inokuti, G. Chamberlain, and S. R. Mielczarek, Phys. Rev. Lett. 21, 1146 (1968); K. J. Miller, S. R. Mielczarek, and M. Krauss, J. Chem. Phys. 51, 26 (1969); S. R. Mielczarek and K. J. Miller, Chem. Phys. Lett. 10, 369 (1971).
[5]K. J. Miller, Int. J. Quantum Chem. 5S, 71 (1971); J. Chem. Phys. 59, 5639 (1973).
[6]K. J. Miller and A. E. S. Green, J. Chem. Phys. 60, 2617 (1974).
[7]J. L. Whitten and M. Hackmeyer, J. Chem. Phys. 51, 5584 (1969).
[8]S. D. Peyerimhoff, R. J. Buenker, W. E. Kammer, and H. Hsu, Chem. Phys. Lett. 8, 129 (1970); R. J. Buenker and S. D. Peyerimhoff, J. Chem. Phys. 53, 1386 (1970).
[9]M. Krauss and S. Mielczarek, J. Chem. Phys. 51, 5241 (1969).
[10]K. J. Miller, J. Chem. Phys. 51, 5235 (1969).
[11]R. A. Bonham, J. Chem. Phys. 36, 3260 (1962).
[12]V. I. Ochkur, Zh. Eksp. Teor. Fiz. 45, 734 (1963) [Sov. Phys.-JETP 18, 503 (1964)].
[13]D. J. T. Morrison and M. R. H. Rudge, Proc. Phys. Soc. Lond. 91, 565 (1967); M. R. H. Rudge, *ibid.* 85, 607 (1965); 86, 763 (1965).